

Self-assembly of C60 monolayer on epitaxially grown, nanostructured graphene on Ru(0001) surface

G. Li, H. T. Zhou, L. D. Pan, Y. Zhang, J. H. Mao et al.

Citation: *Appl. Phys. Lett.* **100**, 013304 (2012); doi: 10.1063/1.3673830

View online: <http://dx.doi.org/10.1063/1.3673830>

View Table of Contents: <http://apl.aip.org/resource/1/APPLAB/v100/i1>

Published by the [American Institute of Physics](#).

Related Articles

Self-assembly of C60 monolayer on epitaxially grown, nanostructured graphene on Ru(0001) surface
[APL: Org. Electron. Photonics 5, 4 \(2012\)](#)

High resolution patterning of nanoparticles by evaporative self-assembly enabled by in situ creation and mechanical lift-off of a polymer template
[Appl. Phys. Lett. 99, 253102 \(2011\)](#)

Morphology-dependent low-frequency Raman scattering in ultrathin spherical, cubic, and cuboid SnO₂ nanocrystals
[Appl. Phys. Lett. 99, 251902 \(2011\)](#)

Bismuth nano-droplets for group-V based molecular-beam droplet epitaxy
[Appl. Phys. Lett. 99, 243113 \(2011\)](#)

Fabrication of horizontal silicon nanowire arrays on insulator by ion irradiation
[AIP Advances 1, 042174 \(2011\)](#)

Additional information on *Appl. Phys. Lett.*

Journal Homepage: <http://apl.aip.org/>

Journal Information: http://apl.aip.org/about/about_the_journal

Top downloads: http://apl.aip.org/features/most_downloaded

Information for Authors: <http://apl.aip.org/authors>

ADVERTISEMENT

**AIPAdvances**

Submit Now

**Explore AIP's new
open-access journal**

- **Article-level metrics
now available**
- **Join the conversation!
Rate & comment on articles**

Self-assembly of C₆₀ monolayer on epitaxially grown, nanostructured graphene on Ru(0001) surface

G. Li, H. T. Zhou, L. D. Pan, Y. Zhang, J. H. Mao, Q. Zou, H. M. Guo, Y. L. Wang, S. X. Du, and H.-J. Gao^{a)}

Institute of Physics, Chinese Academy of Sciences, Beijing, 100190, People's Republic of China

(Received 14 September 2011; accepted 10 December 2011; published online 4 January 2012)

C₆₀ molecules adsorbed on graphene/Ru(0001) substrate were investigated by scanning tunneling microscopy (STM) at 5 K. On high quality substrates, C₆₀ molecules adopt a commensurate growth mode, leading to formation of a supramolecular structure with perfect periodicity and few defects. On under-annealed substrates with imperfections and domains, the molecules form the same closely packed hexagonal structures in spite of underlying corrugations, disorders or steps, indicating a weak molecule-substrate interaction—a conclusion that is also supported by DFT calculations. This system may be beneficial to the fabrication of carbon based devices and of other types of organic functional overlayers. © 2012 American Institute of Physics. [doi:10.1063/1.3673830]

Since its discovery in 1985,¹ C₆₀ has attracted great interest due not only to its unique structural and electronic properties^{2,3} but also to its potential applications in various fields.^{4–8} Extensive studies have been performed on the adsorption and growth properties of C₆₀ on different substrates,^{2,3,9–14} including metal surfaces such as Cu(111),² Ag(100),³ Ag(001),⁹ Au(111)¹⁰, and Ag(111)¹⁰ and semiconductors like silicon¹¹ and GaAs.¹² On these flat surfaces, C₆₀ molecules usually adopt a closely packed hexagonal growth mode.^{2,9,10,12,13} Recently, more attentions have been paid on the adsorption behaviors of C₆₀ on patterned surface structures.^{15–19} While many of these studies focused on trapping C₆₀ molecules by the superstructures, C₆₀ monolayers on periodically corrugated substrates were less investigated.

Based on regularly Moiré structures, a kind of periodically corrugated template—graphene/Ru(0001) (G/Ru in the following) has recently received lots of interest.^{20–25} Here, we report a supramolecular structure of C₆₀ molecules grown on G/Ru surface. The periodic surface potential and the good match between the template and the lattice of adsorbed molecules are the dominant factors for this supramolecular structure. By carefully analyzing C₆₀ growth on under-annealed graphene, we found that the interaction between the C₆₀ molecular layer and the substrate was rather weak. Density functional theory (DFT) study of adsorption energy and the observation of tip-induced rotation of C₆₀ molecules both also support our result. This weak molecule-substrate interaction should be responsible for the continuous and uniform nature of the molecular layer.

The experiments were conducted in an Omicron low temperature STM system under a base pressure better than 1.0×10^{-10} mbar. The G/Ru template was fabricated following the same technique as described in a previous study²¹ except that some of the samples were intentionally under-annealed (~ 1100 K) to create imperfections and domains. C₆₀ (99.5% purity, Aldrich) molecules were evaporated at 600 K onto the samples (kept at room temperature) followed

by annealing at 320 K for 1 h. Then, these samples were transferred to low temperature chamber (~ 5 K) for scanning. Our theoretical calculations were based on DFT by Vienna *ab-initio* simulation package (VASP).²⁶ Projector augmented wave (PAW) potentials²⁷ and local density approximation (LDA)²⁸ for exchange correlation potential were used. The periodic models included a fixed rippling 12×12 graphene super lattice with a C₆₀ molecule adsorbing on three different surface sites (fcc, hcp, atop)²¹ and a vacuum layer of 12 Å. The C₆₀ molecules were fully relaxed until the net force on every atom was less than 0.01 eV/Å. In our calculation, the energy cutoff of the plane-wave basis sets was 400 eV, and a single Γ point was employed for Brillouin zone matrix integrations due to the numerical limitations.

Figure 1(a) shows typical STM topography of a C₆₀ monolayer grown on well-prepared G/Ru surface. The molecules adopt a substrate-commensurate, closely packed hexagonal growth and the bright protrusions are attributed to superimposition of the underlying atop sites of the graphene Moiré structure. A more detailed image is shown in Fig. 1(b). A small (large) rhombus is used to outline the unit cell of the molecular lattice (G/Ru template). This kind of growth was interpreted in two aspects. On the one hand, the corrugated G/Ru surface has a periodical surface potential, which may influence the molecules to some extent in order to achieve minimize energy. On the other hand, given that the distance between two nearest Moiré spots is 3 nm,²¹ almost exactly three times the distance between two neighboring C₆₀ molecules in the solid phase,²⁹ commensurate overlayers can easily form on such a surface. The lattice periodicity is similar to the one reported by Corso *et al.*¹⁵ but with a different supramolecular structure. Also, the defects of the molecular layer on G/Ru surface are much fewer and the molecular film is continuous and uniform even when there are Moiré spots missing (Fig. 1(b)).

Occasionally, especially on the surfaces of under-annealed samples, we also observed incommensurate or disordered growth mode (see Figs. 1(c) and 1(d)). We simply classify the growth modes of C₆₀ into Type A—growth

^{a)}Electronic mail: hjgao@iphy.ac.cn.

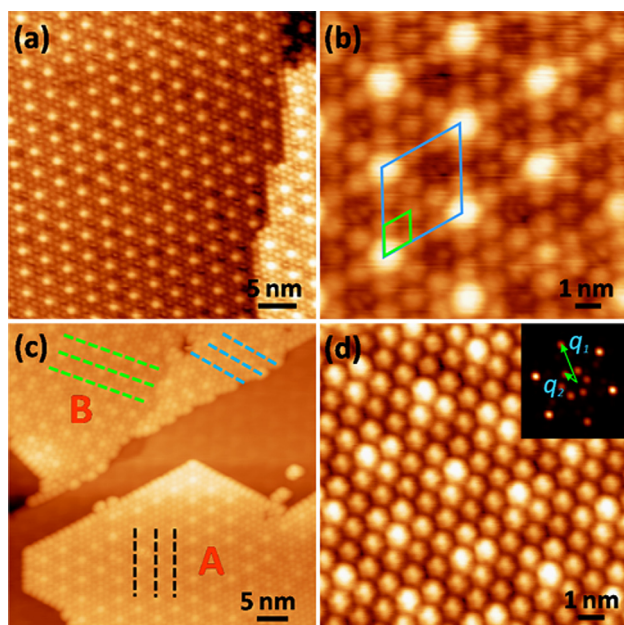


FIG. 1. (Color online) (a) Large-area STM topography of substrate-commensurate growth of C_{60} molecules on G/Ru. Right part is a higher terrace of Ru(0001) surface. (b) Zoom-in image of the supramolecular structure. The unit cells of the underlying substrate and molecular lattice are outlined by large and small rhombuses, respectively. (c) STM image showing both substrate-commensurate (lower right, marked with "A") and substrate-incommensurate (upper left, marked with "B") growth structure of C_{60} molecules on G/Ru. The dotted lines in different colors indicate different domains. (d) Zoom-in image of an incommensurate area. Inset shows its Fourier transformation and the angle between vector q_1 and q_2 is about 26° . Images (a) and (b) were taken from a well prepared sample while (c) and (d) from an under-annealed sample. Scanning parameters: (a) $V_s = -3.0$ V and $I = 0.05$ nA, (b) -2.0 V and 0.1 nA, (c) $+2.0$ V and 0.05 nA, and (d) $+2.0$ V and 0.03 nA.

commensurate with the substrate and Type B—growth that seems disordered. Type B areas occur less frequently and are most likely to appear upon or adjacent to imperfections and domain boundaries, which we suppose to cause their formation. Domain-related Type B growth is incommensurate with the substrate and usually happens when a C_{60} island is stretched across two or more domains (see, e.g., the upper

part of Fig. 1(c)). Hence, this kind of area is sometimes very large in size when C_{60} coverage reached 1 monolayer. In Fig. 1(d), a typical domain-related Type B area is displayed. Since the positions of graphene Moiré spots cannot be clearly resolved in this case, we applied the Fourier transform (FT) to the initial image, as shown in the inset. The outer six points correspond to the C_{60} molecular lattice and the inner ones represent the Moiré pattern's periodicity. By measuring the angle between vectors q_1 and q_2 in the FT image, we found that the two periodic lattices are rotated by 26° with respect to each other. However, this is not the only rotation value we obtained. Among the samples we investigated, such angles range from 4° to 26° , indicating a random relationship between the orientations of the two lattices. This further supports our supposition that incommensurate growth has something to do with domain boundaries, since Moiré pattern domains also have random directions in our samples.

In order to understand more fully the C_{60} molecular layer's continuous nature and freedom from defects, it is helpful to study its growth on the under-annealed samples. Large-area STM topography of C_{60} submonolayer is shown in Fig. 2(a) and here the molecules can be seen to form islands on the G/Ru surface. Around these islands, there are also many randomly isolated molecules appearing as small bright protrusions. As we have mentioned above, the sample in Fig. 2(a) was under-annealed and there were many imperfections and/or defects on its surface which acted as random additional adsorption sites for the adsorbates. Figure 2(b) is an image at lower molecular coverage revealing that the isolated molecules are always found adjacent to areas where Moiré spots are distorted or missing, and a regular Moiré pattern is also shown in Fig. 2(c) for direct comparison. Hence, this kind of isolated adsorption behavior does not suggest a relatively strong C_{60} -substrate interaction or preferential adsorption^{11,22,23} on G/Ru. In fact, on the defect-free areas, we hardly find any isolated molecules. Besides, when samples are heated to 370 K, most C_{60} molecules desorb from the surface, leaving only some that reside near imperfections. The formation of molecular islands on graphene, free of preferential adsorption and with a low desorption

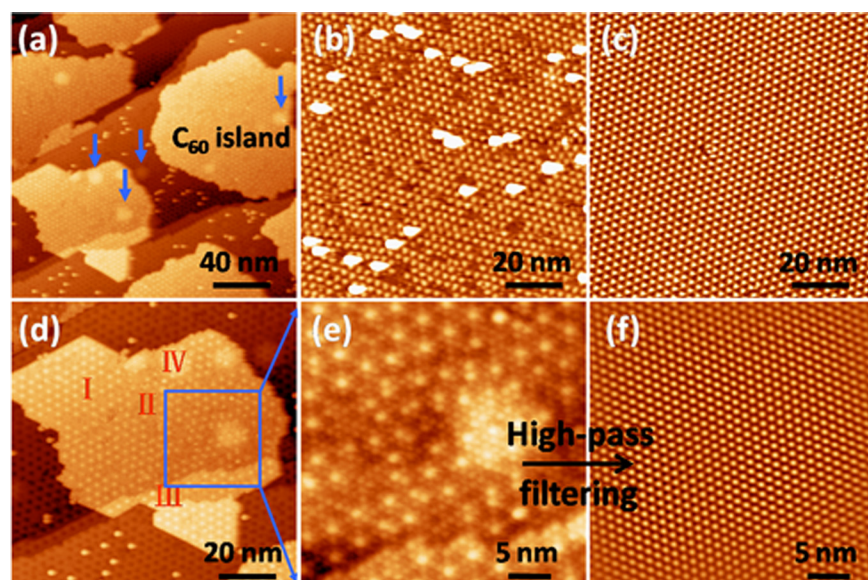


FIG. 2. (Color online) STM topography of C_{60} molecules adsorbed on under-annealed G/Ru surface: (a) Large area STM image showing C_{60} islands and isolated C_{60} molecules. Five larger bright protrusions due to argon gas bubbles are pointed out by blue arrows. (b) Low-coverage image showing defect induced isolated adsorption. (c) Regular Moiré pattern of G/Ru. (d) Zoom-in image of the lower left part of (a). Four kinds of typical template surface conditions are distinguished: (I) regular Moiré pattern, (II) disordered or imperfect areas, (III) steps, and (IV) corrugations. (e) Zoom-in of the area inside the blue square in (d). (f) High-pass filtered image of (e). Scanning parameters: (b) and (c) $V_s = -3.0$ V, $I = 0.05$ nA, (d) and (e) $+3.0$ V, 0.02 nA.

temperature indicate that interactions between adsorbed molecules and the substrate are rather weak. We can also see that Ru substrate has minor influences on C_{60} molecules compared with some previously studied molecules and atoms^{22,23,25} since C_{60} does not show any difference on the adsorption on three different surface sites.

In Fig. 2(a), the larger bright protrusions pointed out by blue arrows are attributed to argon gas bubbles lying a few atomic layers beneath the Ru(0001) surface.³⁰ Thus, the surface in Fig. 2(a) contains four different types of areas: a regular Moiré pattern, imperfections, steps, and argon gas related protrusions. These are labeled in Fig. 2(d) as I, II, III, and IV, respectively. C_{60} molecular island extends over all the four types of surface areas smoothly. To investigate the arrangement of the C_{60} molecules, we further zoom in part of the island (Fig. 2(e)) and find that they also adopt a closely packed hexagonal growth mode. After high-pass filtering, the molecular lattice was made visible in Fig. 2(f). Surprisingly, the lattice is rather well ordered, indicating that the hexagonal packing behavior is retained regardless of underlying imperfections, protrusions, or steps. We emphasize that the height of the steps and protrusions ranges from 0.2~0.3 nm, and the uniform molecular lattice suggests a strong C_{60} - C_{60} interaction compared with the C_{60} -substrate interaction.

With sub-molecular resolution imaging of STM, we further investigated the orientation of C_{60} molecules on G/Ru surfaces. Figure 3(a) shows a C_{60} monolayer under different bias voltages. The intramolecular structure can be resolved and all the molecules are found to share the same orientation, i.e., with a hexagon parallel to the Ru(0001) surface. However, in some cases, the orientations are rather disordered (Figs. 3(b) and 3(c)). Tip-induced molecular rotation was observed during repeated scanning processes, as shown by the circled molecules in Figs. 3(b) and 3(c). The rotation processes under low temperature (5 K) again verified the weak C_{60} -substrate interaction. Our DFT calculations also provided information for quantitative analysis. Given that the Ru substrate has minor effect on C_{60} growth and that the system in Fig. 4 is too large in the DFT calculation, we use a single corrugated graphene layer as the substrate for simplicity. The adsorption energy of C_{60} (hexagon upward) on three

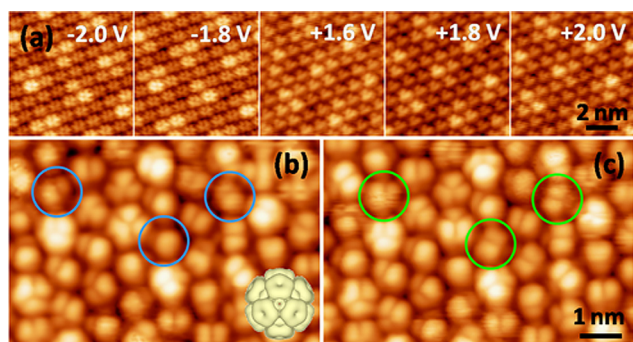


FIG. 3. (Color online) (a) STM topography of C_{60} monolayer under different sample bias voltages with a tunneling current of 0.1 nA. Positive bias corresponds to unoccupied states of the substrate. (b) High resolution image of an orientation disordered area. Inset is the calculated free C_{60} LUMO orbital with a hexagon upward. (c) The same area of (b) after a few cycles of scanning. The rotated molecules are labeled by circles in (b) and (c). Images (b) and (c) are taken at $V_s = +1.5$ V and $I = 0.1$ nA.

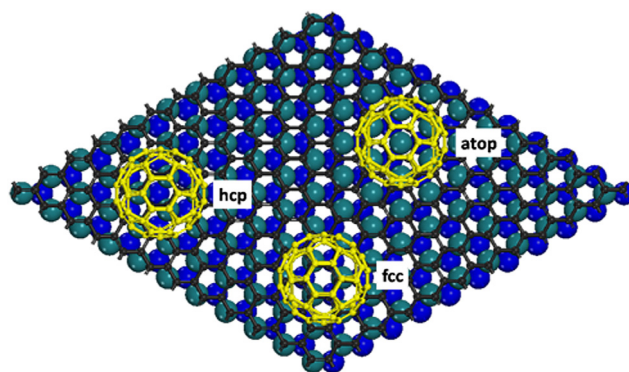


FIG. 4. (Color online) Schematic of the C_{60} /G/Ru system showing the graphene layer (small dark balls), the first Ru layer (large bright balls), and the second Ru layer (large dark balls). C_{60} molecules are placed on three different surface sites in accordance with the commensurate growth mode.

different types of surface sites are -267 meV (atop site), -294 meV (hcp site), and -336 meV (fcc site), respectively, while the interaction energy between two free C_{60} molecules is -514 meV. From these values, we can see the similar adsorption energies of C_{60} molecules on different surface sites and the strong C_{60} - C_{60} interactions finally result in the continuous and defect-free molecular overlayer.

In conclusion, a C_{60} supramolecular structure was fabricated on a G/Ru template. This structure is uniform, continuous, and quite large in size on well-prepared samples. On under-annealed samples however, we found that the interaction between C_{60} molecular film and the substrate is rather weak, but by no means negligible, since it is still enough to guide the commensurate growth of C_{60} molecules. We believe that C_{60} is not the only case in which G/Ru template is suitable for manipulating molecular growth, and that supramolecular structures of other kinds of molecules may also be fabricated using similar techniques. This work may also be helpful for developing future carbon based devices.

This work was financially supported by the NSFC (10834011 and 60976089) and MOST (2009CB929103, 2010CB923004, and 2011CB932700) of China.

¹H. W. Kroto, J. R. Heath, S. C. O'Brien, R. F. Curl, and R. E. Smalley, *Nature* **318**, 162 (1985).

²T. Hashizume, K. Motai, X. D. Wang, H. Shinohara, Y. Saito, Y. Maruyama, K. Ohno, Y. Kawazoe, Y. Nishina, H. W. Pickering *et al.*, *Phys. Rev. Lett.* **71**, 2959 (1993).

³X. H. Lu, M. Grobis, K. H. Khoo, S. G. Louie, and M. F. Crommie, *Phys. Rev. Lett.* **90**, 096802 (2003).

⁴N. S. Sariciftci, D. Braun, C. Zhang, V. I. Srdanov, A. J. Heeger, G. Stucky, and F. Wudl, *Appl. Phys. Lett.* **62**, 585 (1993).

⁵B. Kippelen, S. Yoo, and B. Domercq, *Appl. Phys. Lett.* **85**, 5427 (2004).

⁶R. C. Haddon, A. S. Perel, R. C. Morris, T. T. M. Palstra, A. F. Hebard, and R. M. Fleming, *Appl. Phys. Lett.* **67**, 121 (1995).

⁷H. Park, J. Park, A. K. L. Lim, E. H. Anderson, A. P. Alivisatos, and P. L. McEuen, *Nature* **407**, 57 (2000).

⁸H.-J. Gao, Z. Q. Xue, K. Z. Wang, Q. D. Wu, and S. Pang, *Appl. Phys. Lett.* **68**, 2192 (1996).

⁹M. Grobis, X. Lu, and M. F. Crommie, *Phys. Rev. B* **66**, 161408 (2002).

¹⁰E. I. Altman and R. J. Colton, *Phys. Rev. B* **48**, 18244 (1993).

¹¹J. G. Hou, J. L. Yang, H. Q. Wang, Q. X. Li, C. G. Zeng, H. Lin, W. Bing, D. M. Chen, and Q. S. Zhu, *Phys. Rev. Lett.* **83**, 3001 (1999).

¹²Y. Z. Li, J. C. Patrin, M. Chander, J. H. Weaver, L. P. F. Chibante, and R. E. Smalley, *Science* **252**, 547 (1991).

¹³M. Muntwiler, W. Auwarter, A. P. Seitsonen, J. Osterwalder, and T. Greber, *Phys. Rev. B* **71**, 121402(R) (2005).

- ¹⁴M. Feng, J. Lee, J. Zhao, J. T. Yates, and H. Petek, *J. Am. Chem. Soc.* **129**, 12394 (2007).
- ¹⁵M. Corso, W. Auwarter, M. Muntwiler, A. Tamai, T. Greber, and J. Osterwalder, *Science* **303**, 217 (2004).
- ¹⁶J. A. Theobald, N. S. Oxtoby, M. A. Phillips, N. R. Champness, and P. H. Beton, *Nature* **424**, 1029 (2003).
- ¹⁷H. L. Zhang, W. Chen, H. Huang, L. Chen, and A. T. S. Wee, *J. Am. Chem. Soc.* **130**, 2720 (2008).
- ¹⁸S. Stepanow, M. Lingenfelder, A. Dmitriev, H. Spillmann, E. Delvigne, N. Lin, X. B. Deng, C. Z. Cai, J. V. Barth, and K. Kern, *Nature Mater.* **3**, 229 (2004).
- ¹⁹W. Chen, H. L. Zhang, H. Huang, L. Chen, and A. T. S. Wee, *Appl. Phys. Lett.* **92**, 193301 (2008).
- ²⁰P. W. Sutter, J. I. Flege, and E. A. Sutter, *Nature Mater.* **7**, 406 (2008).
- ²¹Y. Pan, H. G. Zhang, D. X. Shi, J. T. Sun, S. X. Du, F. Liu, and H.-J. Gao, *Adv. Mater.* **21**, 2777 (2009).
- ²²Y. Pan, M. Gao, L. Huang, F. Liu, and H.-J. Gao, *Appl. Phys. Lett.* **95**, 093106 (2009).
- ²³J. H. Mao, H. G. Zhang, Y. H. Jiang, Y. Pan, M. Gao, W. D. Xiao, and H.-J. Gao, *J. Am. Chem. Soc.* **131**, 14136 (2009).
- ²⁴N. A. Pradhan, N. Liu, and W. Ho, *J. Phys. Chem. B* **109**, 8513 (2005).
- ²⁵B. Wang, S. Gunther, J. Winterlin, and M. L. Bocquet, *New J. Phys.* **12**, 043041 (2010).
- ²⁶G. Kresse and J. Furthmuller, *Phys. Rev. B* **54**, 11169 (1996).
- ²⁷P. E. Blochl, *Phys. Rev. B* **50**, 17953 (1994).
- ²⁸J. P. Perdew and A. Zunger, *Phys. Rev. B* **23**, 5048 (1981).
- ²⁹W. Kratschmer, L. D. Lamb, K. Fostiropoulos, and D. R. Huffman, *Nature* **347**, 354 (1990).
- ³⁰M. Gsell, P. Jakob, and D. Menzel, *Science* **280**, 717 (1998).